Available online at www.sciencedirect.com
ScienceDirect
Fluid Phase Equilibria 265 (2008) 84–93
FLUID PHASE EQUILIBRIA
www.elsevier.com/locate/fluid

Study of vapor–hydrate two-phase equilibria

Q.-L. Ma*, G.-J. Chen, C.-F. Ma, L.-W. Zhang

State Key Laboratory of Heavy Oil Processing, China University of Petroleum, Fuxue Road, Changping District, Beijing 102249, China

Received 12 October 2007; received in revised form 27 December 2007; accepted 2 January 2008
Available online 11 January 2008

Abstract

In recent years, the technology of separating gas mixtures by forming hydrate has received increasing recognition, particularly the separation of light-gas mixtures. We performed an experimental and modeling study of systems containing hydrogen, methane, ethane and ethylene, both with and without the thermodynamic promoter tetrahydrofuran (THF) in water. Vapor–hydrate equilibrium data (*P–T–x–y* data) were measured for ($H_2 + CH_4$), ($H_2 + N_2 + CH_4$) and ($CH_4 + C_2H_4$) gas mixtures in the absence and presence of THF. A relatively simple algorithm was used to calculate vapor–hydrate two-phase equilibria. The Patel–Teja equation of state, coupled with a van der Waals–Platteeuw-type hydrate model, was applied to calculate the equilibrium flash of vapor–hydrate phases. The parameters in the hydrate model were determined by correlating the experimental data of hydrate formation conditions. In addition, we predicted the composition of gas mixture in the hydrate phase when structure I and structure II hydrates coexisted in a ($CH_4 + C_2H_6$) gas mixture. The test results indicated that proposed algorithm is adequate for predicting vapor–hydrate equilibria. Accurate predictions of single-stage equilibrium between the vapor and the hydrate phases are important for developing separation technology via hydrate formation.

Keywords: Equilibria; Hydrate; Light-gas; Separation

1. Introduction

The principle of separating gas mixtures via hydrate technology states that, after hydrate formation from a gas mixture, the compositions of gas components are different in the equilibrious vapor and hydrate phases because of the differences in hydrate formation conditions of the gas components; this is comparable with the separation of gas mixtures via partial condensation. This technology is advantageous for separating light-gas mixtures such as ($H_2 + CH_4$) and (C1 + C2), which require deep cooling and consume a huge amount of energy under normal distillation methods. In the chemical and petrochemical and the natural gas industries, the separation of such light-gas mixtures restricts the achievement of high separation efficiency. However, hydrate technology can overcome this problem because hydrate can be formed at ∼0 °C and, theoretically, hydrogen cannot form hydrate, meaning that hydrogen can be separated 100% from the mixture; therefore, material consumption and investment in facilities would be reduced. There have been some studies reported related to the separation technology based on hydrate principles [1–9].

Single-stage hydrate equilibrium is comparable to one-stage equilibrium flash, which directly reflects the separation efficiency of a gas mixture. Equilibrium flash calculations with hydrate phase are important for developing a separation technology via hydrate formation. In the present study, we measured the hydrate formation conditions of a ($CH_4 + C_2H_4$) gas mixtures with tetrahydrofuran (THF) in water and vapor–hydrate equilibrium data of gas mixtures containing hydrogen and ethylene. A simple algorithm was applied to predict single-stage vapor–hydrate equilibria. Two-phase equilibria flash calculation was carried out only to compositions in water-free basis in vapor and hydrate phase. A van der Waals–Platteeuw (vdW–P)-type hydrate model [10,11], combined with the Patel–Teja equation of state (PT EOS) [12], was used to calculate two-phase equilibria.

In certain composition regions of a ($CH_4 + C_2H_6$) gas mixture, structure I (sI) and structure II (sII) hydrates coexist in equilibrium [13,14], whereas pure methane and ethane usually form sI hydrate. It is widely assumed that, if two sI hydrate producers such as methane and ethane are mixed, the resulting

* Corresponding author. Tel.: +86 10 89733252.
E-mail address: maql@cup.edu.cn (Q.-L. Ma).

0378-3812/$ – see front matter © 2008 Elsevier B.V. All rights reserved.
doi:10.1016/j.fluid.2008.01.001

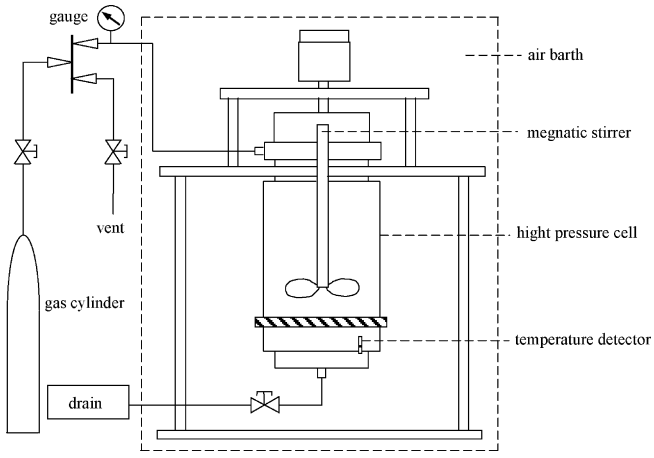

Fig. 1. The schematic of experimental apparatus.

hydrate will always be sI. However, the results of calculations of composition in the hydrate phase are not always consistent with experimental data in this respect; therefore, calculations should be performed assuming that two hydrate structures coexist. A difficulty arises in terms of how to determine the ratio of sI:sII hydrate formation in the solid phase. The hydrate formation kinetic model was used to control this ratio in this study. The tests were aimed mainly at systems involved in the separation of cracking gas and oil processing. The results show that the prediction of vapor–hydrate equilibria is of significance to practical operation.

2. Experimental study

2.1. Experimental apparatus

The experimental apparatus used to measure the hydrate formation conditions in this study has been described in detail in previous articles from this laboratory [15–17]. The apparatus consisted of a cylindrical transparent sapphire cell (2.54 cm in diameter, effective volume of 60 cm^3) installed in an air bath and equipped with a magnetic stirrer for accelerating the equilibrium process. The formation and dissociation of the hydrate crystals in the solution were observed directly through the transparent cell wall. The accuracy of temperature and pressure measurement was ±0.2 K and ±0.025 MPa, respectively.

The experimental apparatus used to measure vapor–hydrate equilibria consisted mainly of a cylindrical stainless steel cell with an effective volume of 256 cm^3 (Fig. 1). The accuracy of temperature and pressure measurement was within ±0.1 K and ±0.025 MPa, respectively.

2.2. Materials and preparation of samples

Analytical-grade methane (99.99%), ethylene (99.5%) and hydrogen (99.99%), supplied by Beifen Gas Industry Corporation, were used to prepare the feed gas mixtures. The composition of gas mixtures was analyzed using a Hewlett-Packard gas chromatograph (HP 6890). The THF used for preparing the aqueous solution was supplied by Beijing Reagents Corporation. An electronic balance with a precision of ±0.1 mg was used to prepare the aqueous solution with the required concentration of THF.

2.3. Experimental procedures

2.3.1. Hydrate formation conditions

First, the transparent cell was washed with deionized water and then rinsed three times with the prepared THF aqueous solution. After the cell was thoroughly cleaned, ∼10 cm^3 of the prepared aqueous solution was added to the cell, which was then installed in the air bath. The vapor space of the cell was then purged four times with the prepared gas mixture to ensure the absence of air. The temperature of the air bath was then adjusted to the given value and the cell was charged with the gas mixture.

The pressure in the cell was raised to ∼1 MPa higher than the estimated equilibrium pressure via the floating piston. When a trace of hydrate crystal was observed, the pressure was reduced gradually to allow the hydrate crystals decompose slowly. When

Table 1
Hydrate formation conditions of (methane + ethylene) gas mixtures from 6 mol% THF aqueous solution

Composition of gas mixture (mol%)	T (K)	P (MPa)
11.63% CH_4 + 88.37% C_2H_4	277.7	0.48
	279.7	0.93
	281.2	1.36
	282.7	1.90
23.85% CH_4 + 76.15% C_2H_4	278.2	0.41
	280.2	0.73
	281.7	1.04
	283.2	1.39
	284.7	1.82
	286.7	2.49
42.88% CH_4 + 57.12% C_2H_4	278.2	0.28
	280.2	0.49
	282.7	0.85
	285.2	1.31
	288.2	2.05
70.65% CH_4 + 29.35% C_2H_4	277.7	0.17
	279.7	0.31
	281.7	0.49
	283.7	0.72
	286.2	1.09
	288.2	1.46
86.24% CH_4 + 13.76% C_2H_4	278.2	0.17
	280.2	0.30
	282.2	0.46
	284.7	0.77
	286.7	1.06
	288.2	1.31
93.72% CH_4 + 6.28% C_2H_4	278.2	0.16
	280.2	0.28
	282.2	0.43
	284.2	0.66
	286.2	0.94
	288.2	1.26

Table 2
Vapor–hydrate equilibrium data of ($CH_4(1) + C_2H_4(2)$) gas mixtures with 6 mol% THF aqueous solution ($T = 274.15$ K)

P (MPa)	W (mol%)	z_2 (mol%)	y_2 (mol%)	x_2 (mol%)
1.12	89	34.79	56.61	21.97
1.29	89		59.27	23.31
1.46	88.5		60.05	24.19
1.57	87.5		57.29	22.38
1.74	86.5		55.03	20.57
1.89	85		52.15	19.42
1.31	90	15.90	32.08	11.02
1.44	89.5		31.03	10.64
1.62	88		28.26	9.46
1.81	87		26.68	8.79

Table 3
Vapor–hydrate equilibrium data of ($CH_4(1) + H_2(2)$) gas mixtures with pure water ($T = 274.35$ K)

P (MPa)	W (mol%)	z_2 (mol%)	y_2 (mol%)	x_2 (mol%)
3.82	70	14.40	23.98	1.07
4.74	72	22.59	38.61	1.46
5.14	62	31.09	43.62	3.25
5.57	52	39.95	49.38	3.41

Table 4
Vapor–hydrate equilibrium data of ($CH_4(1) + H_2(2)$) gas mixtures with 1 mol% THF aqueous solution ($T = 278.15$ K)

P (MPa)	W (mol%)	z_2 (mol%)	y_2 (mol%)	x_2 (mol%)
1.42	83	34.74	50.21	2.09
2.42	83.5	35.38	57.88	3.43
3.65	83.5	34.05	56.65	4.44

all the hydrate crystals disappeared, the pressure of the system was raised again by a small pressure-step of 0.05 MPa until the hydrate crystal appears again. Maintain the system temperature and pressure for 6 h, if the hydrate crystals disappeared during this period, the pressure of the system was raised slightly until a trace of hydrate crystals appeared again. When the hydrate crystals are kept in the cell after 6 h, the system pressure is taken as the equilibrium hydrate formation pressure at the given temperature. The above procedure was repeated for a series of temperatures.

2.3.2. Vapor–hydrate equilibrium

Preparation for the measurement of vapor–hydrate equilibrium was the same as above. After temperature stabilization, the gas sample was charged into the stainless steel cell until the given pressure was achieved. Subsequently, hydrate nucleation was started with agitation of the magnetic stirrer. The system pressure was kept stable for 4 h and the vapor–hydrate equilibrium was then established. The vapor phase was sampled and analyzed at least three times using the gas chromatograph. The average values were then taken as the compositions of the vapor phase. The concentrations of components in the hydrate phase were obtained by analyzing the compositions of gas released from dissociated hydrate using the gas chromatograph.

Table 5
Vapor–hydrate equilibrium data of a ($CH_4(1) + H_2(2)$) gas mixture with 5 mol% THF aqueous solution ($T = 278.65$ K)

P (MPa)	W (mol%)	z_2 (mol%)	y_2 (mol%)
6.21	60	70.08	78.90
5.92	68		82.77
5.61	76		87.34
5.42	78		90.41

Table 6
Vapor–hydrate equilibrium data of a ($H_2(1) + N_2(2) + CH_4(3)$) gas mixture with 1 mol% THF aqueous solution ($T = 274.95$ K, $z_1 = 61.43$ mol%, $z_2 = 10.99$ mol%, $z_3 = 27.58$ mol%)

P (MPa)	W (mol%)	y_1 (mol%)	y_2 (mol%)	y_3 (mol%)
7.42	35	62.71	11.40	25.89
7.08	43	66.29	11.22	22.49
6.87	67	73.96	10.03	15.20
6.68	72	76.69	10.43	12.98
6.43	72.5	77.67	10.39	11.94
6.00	73	78.88	9.98	11.14

2.4. Experimental results

2.4.1. Hydrate formation conditions

Some experimental studies of hydrate formation conditions have been performed previously by this laboratory [15–18]. In this study, we complementally measured the hydrate formation pressures of a ($CH_4 + C_2H_4$) system from a THF aqueous solution. The hydrate formation data measured are listed in Table 1.

2.4.2. Vapor–hydrate equilibrium

In this study, the compositions of gas mixtures in the vapor and hydrate phases were both in water- and THF-free basis. z_2, x_2 and y_2 represent the concentration of ethylene or hydrogen in feed gas (the prepared gaseous mixture sample), the hydrate phase and the vapor phase, respectively. W represents the mole fraction of water or aqueous solution in the feed (gas + water) mixture.

We measured the vapor–hydrate equilibria of a ($CH_4 + C_2H_4 + THF$) system and systems containing hydrogen in the absence and presence of THF, which are relevant to the oil- and gas-processing and petrochemical industries. Table 2 shows the equilibrium data for a ($CH_4 + C_2H_4$) gas mixture with 6 mol% THF aqueous solution. The equilibrium data for ($CH_4 + H_2$) gas mixtures with pure water and THF aqueous solution are presented in Tables 3–5. The operation

Table 7
Vapor–hydrate equilibrium data of a ($H_2(1) + N_2(2) + CH_4(3)$) gas mixture with 5 mol% THF aqueous solution ($T = 274.95$ K, $z_1 = 59.52$ mol%, $z_2 = 35.79$ mol%, $z_3 = 4.69$ mol%)

P (MPa)	W (mol%)	y_1 (mol%)	y_2 (mol%)	y_3 (mol%)
7.00	62	68.89	29.00	2.11
6.89	67	70.10	28.34	1.56
6.55	70	75.80	20.95	3.15

Table 8
Parameters in Eq. (4) (structure I)

Substance	Small cavity			Large cavity		
	A_{mj} ($\times 10^3$ K kPa^{-1})	B_{mj} ($\times 10^{-3}$ K)	D_{mj} ($\times 10^{-6}$ K^2)	A_{mj} ($\times 10^3$ K kPa^{-1})	B_{mj} ($\times 10^{-3}$ K)	D_{mj} ($\times 10^{-6}$ K^2)
C_2H_4	0.000922	3.17954	0.05203	0.016280	3.65159	0.04236
H_2	0.0005380	2.45183	0.26414	0.0	0.0	0.0
THF	0.0	0.0	0.0	0.0	0.0	0.0

Table 9
Parameters in Eq. (4) (structure II)

Substance	Small cavity			Large cavity		
	A_{mj} ($\times 10^3$ K kPa^{-1})	B_{mj} ($\times 10^{-3}$ K)	D_{mj} ($\times 10^{-6}$ K^2)	A_{mj} ($\times 10^3$ K kPa^{-1})	B_{mj} ($\times 10^{-3}$ K)	D_{mj} ($\times 10^{-6}$ K^2)
C_2H_4	0.0000192	2.85010	0.04363	1.627772	3.35852	0.01894
H_2	0.0005497	1.89901	0.22534	0.0	0.0	0.0
THF	0.0	0.0	0.0	6.568961	4.979	0.02840

temperature is raised following the addition of THF, which saves refrigeration energy.

Methane is enriched in the hydrate phase. Theoretically, methane released from hydrate should be 100% pure because hydrogen cannot form hydrate. However actually in the presence of help guests such as methane in this study, very few amount of hydrogen can occupy small cavity whereas pure hydrogen cannot form hydrate. Therefore, pure methane cannot be obtained. Considering that refinery cracking gas and industrial gas generally contain nitrogen, we measured synthetic-gas mixtures containing nitrogen; the data are shown in Tables 6 and 7, where only the compositions of the vapor phase were measured. Hydrogen was separated effectively from the gas mixture through the formation of hydrate gas (Tables 6 and 7). However, further research is required to improve the separation of nitrogen from methane.

3. Modeling study

3.1. Thermodynamic model

The equilibrium criterion is expressed as follows:

$$\Delta\mu_w^H = \Delta\mu_w^W \tag{1}$$

where $\Delta\mu_w^H$ and $\Delta\mu_w^W$ denote the difference in chemical potential between empty hydrate lattice and water in the hydrate phase and in the aqueous phase, respectively.

The vdW–P hydrate model [19] was used to calculate $\Delta\mu_w^H$, which is expressed as follows:

$$\Delta\mu_w^H = -RT\sum_{m=1}^{2} v_m \ln(1-\theta_m) \tag{2}$$

where v_m denotes cavity number per water molecule and θ_m denotes the fractional filling of cavity m by guest molecules. According to the Langmuir adsorption theory, θ_m can be obtained by

$$\theta_m = \frac{\sum C_{mj} f_j}{1+\sum C_{mj} f_j} \tag{3}$$

where f_j denotes the fugacity of gas species j and where C_{mj} is the Langmuir constant of j in a type-m cavity.

The Du–Guo model [20] was used to estimate C_{mj}:

$$C_{mj}(T) = \frac{A_{mj}}{T}\exp\left(\frac{B_{mj}}{T}+\frac{D_{mj}}{T^2}\right) \tag{4}$$

The parameters A_{mj}, B_{mj} and D_{mj} for ethylene, hydrogen and THF were determined by fitting the experimental data of hydrate formation conditions (Tables 8 and 9) (see Ref. [11] for parameters for other substances).

$\Delta\mu_w^W$ was calculated as follows:

$$\frac{\Delta\mu_w^W}{RT} = \frac{\Delta\mu_w^0(T_0,0)}{RT_0} + \int_0^P \frac{\Delta V_w}{RT}\mathrm{d}P - \int_{T_0}^{T} \frac{\Delta h_w}{RT^2}\mathrm{d}T - \ln a_w \tag{5}$$

$$\Delta h_w = \Delta h_w^0 + \int_{T_0}^{T} \Delta C_{Pw}\,\mathrm{d}T \tag{6}$$

$$\Delta C_{Pw} = \Delta C_P^0 + b(T-T_0) \tag{7}$$

The constants in Eqs. (5)–(7) applied in this work are listed in Table 10 [21]. The activity of water in the aqueous phase (a_w) is equal to 1 for pure water. The Wilson activity model [22] was

Table 10
Hydrate constants in Eqs. (5)–(7) (T_0 = 273.15 K)

Constant	Structure I	Structure II
$\Delta\mu_w^0$ (J mol^{-1})	1120	931
Δh_w^0 (J mol^{-1})	−4297	−4611
ΔV_w (mL mol^{-1})	4.5959	4.99644
ΔC_{Pw} (J mol^{-1} K^{-1})	$-34.583+0.189(T-T_0)$	$-36.861+0.181(T-T_0)$

Table 11
Comparison of experimental and correlated hydrate formation pressures in pure water

System	P-range (MPa)	T-range (K)	AADP[a] (%)	N_p	Data source
C_2H_4	0.665–3.21	273.7–283.2	4.1807	10	[4]
34.09% CH_4 + 65.91% C_2H_4	0.784–3.115	278.2–288.2	4.2005	5	[4]
85.69% CH_4 + 14.31% C_2H_4	1.800–4.640	278.2–288.2	2.1643	4	[4]
36.18% H_2 + 63.82% CH_4	4.56–6.73	274.3–285.2	1.5903	5	[26]
22.13% H_2 + 77.87% CH_4	3.82–5.44	274.3–285.2	1.0477	5	[26]
87.22% H_2 + 12.78% C_3H_8	2.3–4.1	275.2–278.3	3.7916	4	[26]
81.64% H_2 + 18.36% C_3H_8	1.36–2.82	274.2–278.1	4.4187	5	[26]
77.10% H_2 + 22.90% C_3H_8	0.95–2.5	274.2–278.2	0.0993	5	[26]
Overall			2.6866		

[a] $\mathrm{AADP}(\%) = (1/N)\sum_j^{N_p} \left|(P_{Cal} - P_{Exp})/P_{Exp}\right|_j \times 100.$

used to calculate a_w for THF aqueous solution. The PT EOS was applied to calculate vapor-phase properties.

3.2. Algorithm for vapor–hydrate-phase equilibrium calculations

With the gases of low solubility, vapor–hydrate two-phase equilibrium calculations can be performed on a water-free basis only if the amount of water in the vapor phase is ignored, which is similar to vapor–liquid two-phase equilibrium calculations. Therefore, the overall and component material-balance equations are expressed as follows:

$$F = V + H \tag{8}$$

$$Fz_i = Vy_i + Hx_i \tag{9}$$

where F, V and H denote the mole fraction of feed, vapor phase and hydrate phase in equilibrium, respectively; z_i, y_i and x_i denote the composition (mole fraction) of feed, vapor phase and hydrate phase, respectively. Defined e as the mole fraction of the vapor phase in the flash, Eq. (9) can be rewritten as follows:

$$z_i = ey_i + (1 - e)x_i \tag{10}$$

or

$$y_i = \frac{z_i - (1 - e)x_i}{e} \tag{11}$$

Based on the vdW–P hydrate model, the amount of guest component i in hydrate per water molecule (x_i') should be

$$x_i' = \nu_1 \frac{C_{i1} f_i}{1 + \sum_j C_{j1} f_j} + \nu_2 \frac{C_{i2} f_i}{1 + \sum_j C_{j2} f_j} \tag{12}$$

Thus, the mole fraction of i in the hydrate phase can be expressed as

$$x_i = \frac{x_i'}{\sum x_i'} \tag{13}$$

Generally, independent variables are given as follows:

Independent variable	Number of variable
F	1
z_i	$c - 1$
P	1
T	1
W	1
Σ	$c + 3$

where c is the number of components of the gas mixture, F denotes the flux of feed on a water-free basis and W is the mole fraction of water or aqueous solution in the feed (gas + water) mixture. The amount of water in the feed mixture determines the fraction of hydrate phase and its composition. The fraction of phase (e) is related to W as follows in the case of pure water:

$$e = 1 - \frac{W}{1 - W} \sum_{i=1}^{c} \left(\nu_1 \frac{C_{1i} f_i}{1 + \sum_j C_{j1} f_j} + \nu_2 \frac{C_{2i} f_i}{1 + \sum_j C_{j2} f_j} \right) \tag{14}$$

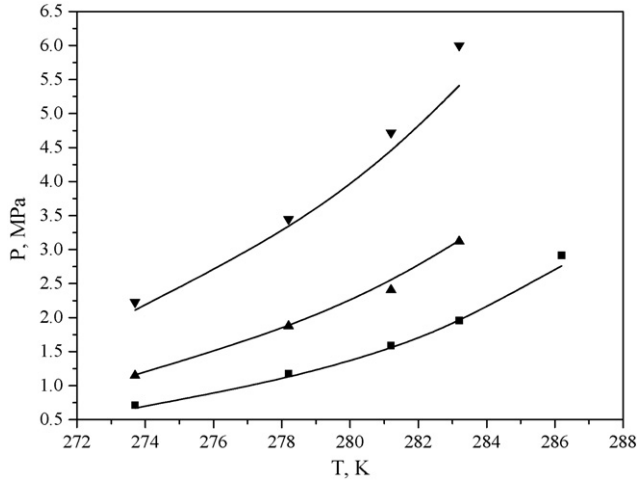

Fig. 2. Comparison of predicted hydrate formation pressures with experimental data [4] of ($CH_4 + C_2H_4$) gas mixtures with pure water. (■) Experimental data, 5.60% CH_4 + 94.40% C_2H_4; (▲) experimental data, 64.28% CH_4 + 35.72% C_2H_4; (▼) experimental data, 92.87% CH_4 + 7.13% C_2H_4; (—) calculation results.

Table 12
Comparison of experimental and correlated hydrate formation pressures from 6 mol% THF aqueous solution

System	*P*-range (MPa)	*T*-range (K)	AADP[a] (%)	N_p
11.63% CH_4 + 88.37% C_2H_4	0.480–1.900	277.7–282.7	3.3749	4
23.85% CH_4 + 76.15% C_2H_4	0.410–2.490	278.2–286.7	2.8285	6
42.88% CH_4 + 57.12% C_2H_4	0.280–2.050	278.2–288.2	4.5331	5
70.65% CH_4 + 29.35% C_2H_4	0.170–1.460	277.7–288.2	6.5604	6
86.24% CH_4 + 13.76% C_2H_4	0.170–1.310	278.2–288.2	4.8212	6
93.72% CH_4 + 6.28% C_2H_4	0.160–1.260	278.2–288.2	4.9579	6
Overall			4.5127	

If there is an inhibitor or promoter in the aqueous phase, e is related to W as follows:

$$e = 1 - \frac{W(1 - x_{inh})}{1 - W} \sum_{i=1}^{c} \left(\nu_1 \frac{C_{1i} f_i}{1 + \sum_j C_{j1} f_j} + \nu_2 \frac{C_{2i} f_i}{1 + \sum_j C_{j2} f_j} \right) \quad (15)$$

where x_{inh} denotes the mole fraction of inhibitor or promoter in water.

The calculation procedure can be summarized as follows:

(i) Input specified temperature (T), pressure (P) and composition of feed on a water-free basis (z_i). Input water mole fraction of feed (gas + water) mixture (W).
(ii) Based on T and z_i, calculate hydrate formation pressure (P_H). Judge whether $P > P_H$ is satisfied. If not, the hydrate phase will not be formed, so omit the two-phase flash calculation. If so, the hydrate phase is present, so proceed to subsequent steps.
(iii) Based on T, P_H and z_i, calculate the initial value of composition of the hydrate phase (x_i). Calculate the initial value of the mole fraction of vapor phase (e) using Eq. (14).
(iv) Calculate the mole fraction of each component in the vapor phase (y_i) using Eq. (11).
(v) Based on T, P and y_i, calculate the vapor-phase fugacity (f_i) using PT EOS.
(vi) Calculate the mole fraction of each component in the hydrate phase (x_i) from f_i using Eqs. (12) and (13).
(vii) Calculate the new value of the mole fraction of vapor phase (e') using Eq. (14).
(viii) Judge whether the difference between e' and e meets the precision requirement ($|(e' - e)/e| < 10^{-3}$) If not, adjust e to e' and repeat steps ((iv)–(viii)) until the preset precision is satisfied.

The calculation procedure is the same for THF aqueous solution except that, in this case, the activity of water in Eq. (5) is not equal to 1. We applied the Wilson activity model to calculate the activities of water and THF in the aqueous phase. THF can form only sII hydrate and occupy only large cavities. Its hydrate model parameters are listed in Tables 7 and 8.

The systems of ($CH_4 + C_2H_6$) mixtures require more attention. Pure methane and ethane usually form sI hydrate. However, their mixtures will form sI and sII hydrates simultaneously when methane is in certain composition regions [13,14]. Where sI and sII hydrates coexist, the key problem is determining the ratio of formation of the two structure hydrates.

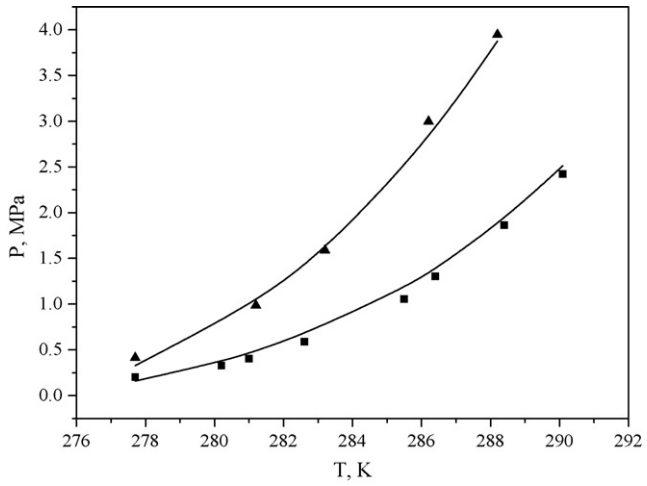

Fig. 3. Comparison of predicted hydrate formation pressures with experimental data [18] of ($H_2 + CH_4$) gas mixtures with 6 mol% THF aqueous solution. (■) Experimental data, 34.74% H_2 + 65.26% CH_4; (▲) experimental data, 69.71% H_2 + 30.29% CH_4; (—) calculation results.

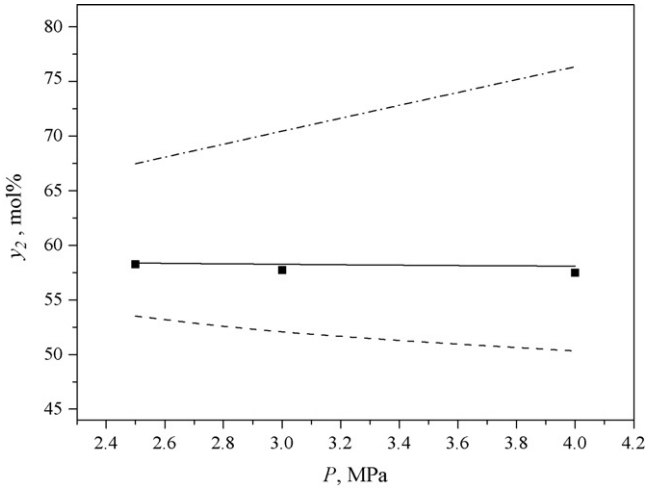

Fig. 4. Comparison of calculated and experimental mole fraction of C_2H_6 in the vapor phase for a (39.89% CH_4 + 60.11% C_2H_6) gas mixture with pure water (T = 274.15K). (■) Experimental data [8]; (—) calculation result (sI + sII); (- - -) calculation result (sI); (— · — · —) calculation result (sII).

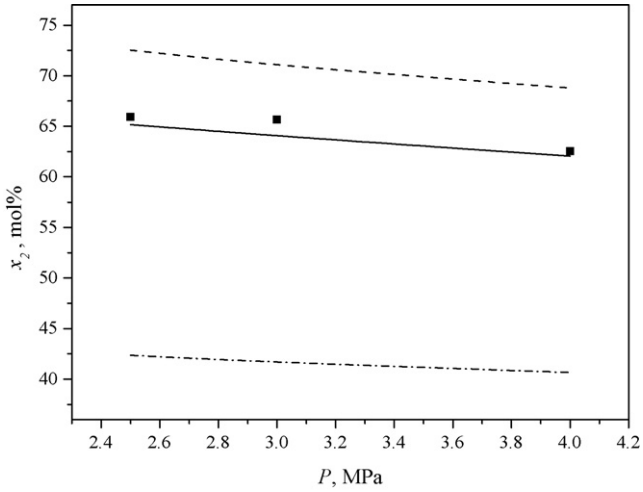

Fig. 5. Comparison of calculated and experimental mole fraction of C_2H_6 in the hydrate phase for a (39.89% CH_4 + 60.11% C_2H_6) gas mixture with pure water (T = 274.15 K). (■) Experimental data [8]; (—) calculation result (sI + sII); (- - -) calculation result (sI); (— · — · —) calculation result (sII).

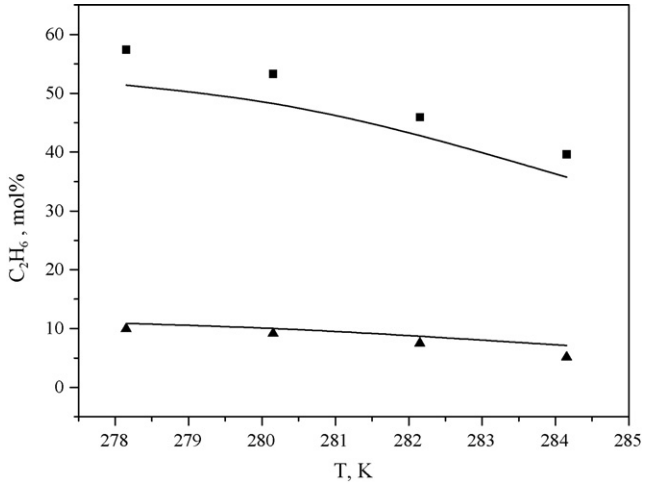

Fig. 6. Comparison of calculated and experimental mole fraction of C_2H_6 in the vapor and hydrate phase for a (75.61% CH_4 + 24.39% C_2H_6) gas mixture with 6 mol% THF aqueous solution (P = 2 MPa). (■) Experimental data [8] (in vapor phase); (▲) experimental data [8] (in hydrate phase); (—) calculation results.

Following hydrate formation kinetics, the hydrate formation rate can be expressed as follows:

$$\frac{dn}{dt} = K\left[\exp\left(-a\frac{\Delta G}{RT}\right) - 1\right] \tag{16}$$

where a is a dimensionless parameter (a = 8.653) and K is the reaction rate constant. Considering that hydrate growth is controlled mainly by mass transfer between gas–liquid interfaces and the diffusion of gas molecules in the liquid phase [23,24], we applied the same K value to two different structure hydrates; G denotes Gibbs free energy. Consequently, the ratio of formation of the two structure hydrates (η) can be determined as follows:

$$\eta = \frac{n^{II}}{n^{I}} = \frac{[\exp(-a/(\Delta G^{II}/RT)) - 1]}{[\exp(-a/(\Delta G^{I}/RT)) - 1]} \tag{17}$$

$$\eta = \frac{\exp\left[a\sum_i \nu_i^{II} \ln\left(1 - \sum_j \theta_{ji}^{II}\right)\right] - 1}{\exp\left[a\sum_i \nu_i^{I} \ln\left(1 - \sum_j \theta_{ji}^{I}\right)\right] - 1} \tag{18}$$

where n^I and n^{II} denote the amount of sI and sII hydrates in the hydrate phase, respectively; the fraction of cavity i occupied by gas component j in two structure hydrates, θ_{ji}^{I} and θ_{ji}^{II}, can be calculated using Eq. (3).

The mole fraction of gas component i in sI and sII hydrates, x_i^I and x_i^{II}, can be calculated using Eqs. (12) and (13). Therefore, the total mole fraction of component i in the hydrate phase can be obtained as follows:

$$x_i = \frac{n^I x_i^I + n^{II} x_i^{II}}{n^I + n^{II}} = \frac{x_i^I + \eta x_i^{II}}{1 + \eta} \tag{19}$$

For predicted calculations of a ($CH_4 + C_2H_6$) gas mixture, if the concentration of methane is in the range 0.4–0.75 mol% [13,25] and the system pressure is higher than the formation pressure of sI and sII hydrates, the composition of the hydrate phase should be calculated by Eqs. (18) and (19).

3.3. Results and discussion

3.3.1. Determination of hydrate model parameters

Tables 11 and 12 show the calculation results of the hydrate formation conditions for systems containing hydrogen and ethylene in pure water and in THF aqueous solution, respectively; these results are used to determine the parameters listed in Tables 8 and 9. The predicted results for ($CH_4 + C_2H_4$) gas mixtures with pure water are shown in Fig. 2. The hydrate formation pressures are heightened along with the increases of the concentration of methane in mixtures. The predicted results for ($H_2 + CH_4$) gas mixtures with aqueous solution of 6 mol% THF are shown in Fig. 3. The predictions are consistent with the experimental data.

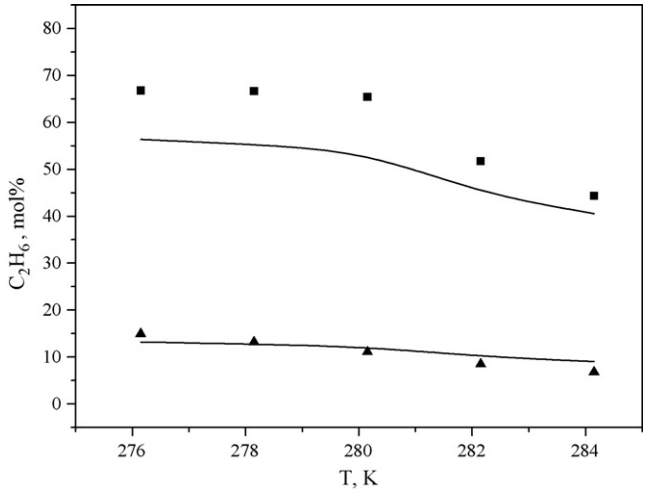

Fig. 7. Comparison of calculated and experimental mole fraction of C_2H_6 in the vapor and hydrate phase for a (75.61% CH_4 + 24.39% C_2H_6) gas mixture with 6 mol% THF aqueous solution (P = 3 MPa). (■) Experimental data [8] (in vapor phase); (▲) experimental data [8] (in hydrate phase); (—) calculation results.

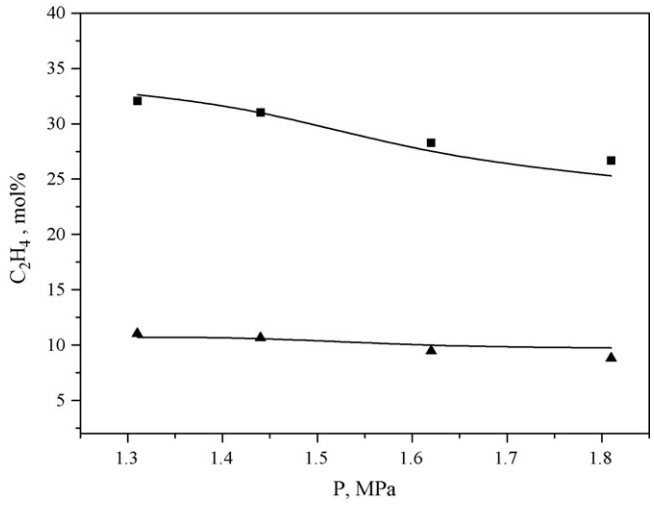

Fig. 8. Comparison of calculated and experimental mole fraction of C_2H_4 in the vapor and hydrate phase for a (84.1% CH_4 + 15.9% C_2H_4) gas mixture with 6 mol% THF aqueous solution (T = 274.15 K). (■) Experimental data (in vapor phase); (▲) experimental data (in hydrate phase); (—) calculation results.

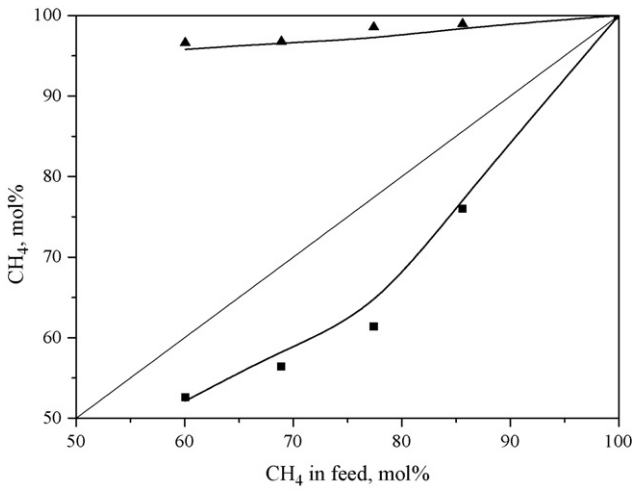

Fig. 10. Comparison of calculated and experimental mole fraction of CH_4 in the vapor and hydrate phase for (CH_4 + H_2) gas mixtures with pure water (T = 274.35 K). (■) Experimental data (in vapor phase); (▲) experimental data (in hydrate phase); (—) calculation results.

3.3.2. *Vapor–hydrate two-phase equilibrium calculation*

The proposed algorithm of vapor–hydrate flash calculation was used to predict the separation result of gas mixtures containing methane, ethane, hydrogen and ethylene.

3.3.2.1. (C1 + C2) systems. For (CH_4 + C_2H_6) gas mixtures with pure water, the equilibrium calculation was first carried out supposing that only sI or sII hydrates formed. The calculation deviation was great. The average deviation of the mole fraction of ethane was 9.8% for sI and 29.7% for sII, respectively. The predicted mole fraction of ethane in sI hydrate was greater than in the experimental data, whereas the mole fraction in sII hydrate was less than in the experimental data. It was calculated again supposing that sI and sII hydrates coexist (Figs. 4 and 5). The predicted results improved greatly. The average deviation of the mole fraction of ethane was 1.1%.

From the separation results of gas mixture with pure water, it can be seen that the separation effect is not satisfactory and requires high operational pressure, which restricts the application of hydrate technology to practical production. To improve separation conditions and to heighten efficiency, it is necessary to add some quantity of promoter to water, and THF is currently considered a suitable thermodynamic promoter.

Figs. 6 and 7 show the calculation results of the mole fraction of ethane in the vapor and hydrate phases for a (75.61% CH_4 + 24.39% C_2H_6) gas mixture with an aqueous solution containing 6 mol% THF. The separation efficiency of ethane was enhanced compared with in the absence of THF (Figs. 4 and 5), and the operation pressures were lowered and temperatures were raised to some extent. When THF was added to the aqueous phase, ethane was enriched in the vapor phase instead of in the hydrate phase (Fig. 5) because THF forms hydrate more eas-

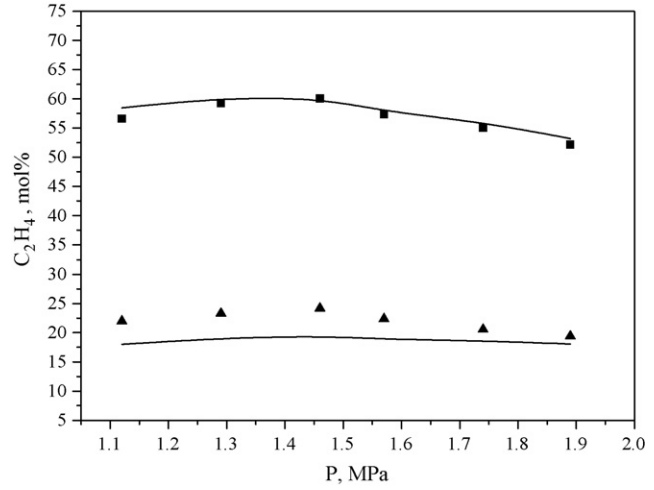

Fig. 9. Comparison of calculated and experimental mole fraction of C_2H_4 in the vapor and hydrate phase for a (65.21% CH_4 + 34.79% C_2H_4) gas mixture with 6 mol% THF aqueous solution (T = 274.15 K). (■) Experimental data (in vapor phase); (▲) experimental data (in hydrate phase); (—) calculation results.

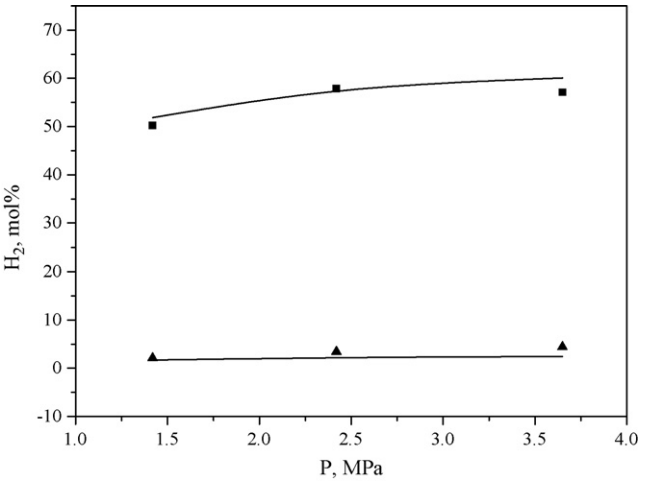

Fig. 11. Comparison of calculated and experimental mole fraction of H_2 in the vapor and hydrate phase for (CH_4 + H_2) gas mixtures with 1 mol% THF aqueous solution (T = 278.15 K). (■) Experimental data (in vapor phase); (▲) experimental data (in hydrate phase); (—) calculation results.

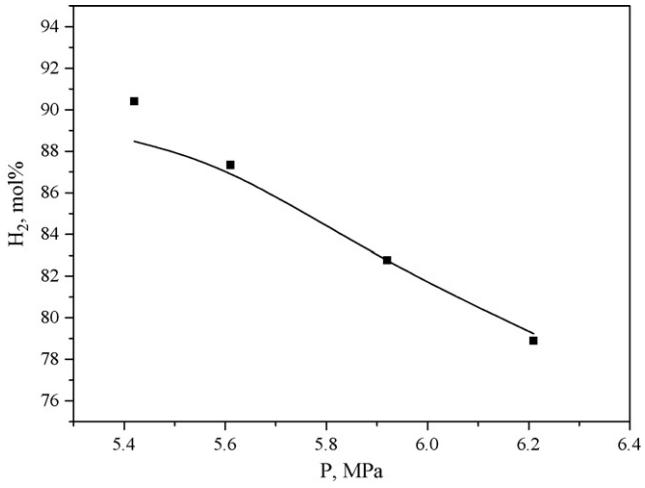

Fig. 12. Comparison of calculated and experimental mole fraction of H_2 in the vapor phase for a (29.92% CH_4 + 70.08% H_2) gas mixture with 5 mol% THF aqueous solution (T = 278.65 K). (■) Experimental data; (—) calculation result.

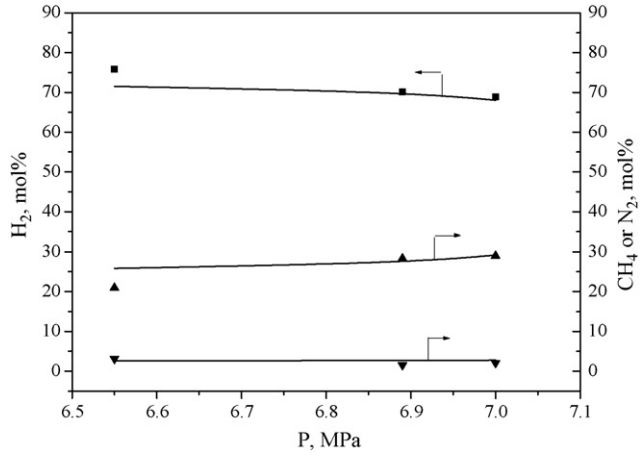

Fig. 14. Comparison of calculated and experimental composition of a (H_2 + N_2 + CH_4) gas mixture in the vapor phase with 5 mol% THF aqueous solution (T = 277.55 K). (■) Experimental data (H_2); (▲) experimental data (N_2); (▼) experimental data (CH_4); (—) calculation results.

ily than it does ethane. The same results can be obtained for a (CH_4 + C_2H_4) gas mixture (Figs. 8 and 9, Table 2).

3.3.2.2. Systems containing hydrogen. We tested systems containing hydrogen in the absence and presence of THF. The predicted results are shown in Figs. 10–14.

Fig. 10 shows the equilibrium separation results for a (CH_4 + H_2) gas mixture with pure water. The predicted results for (CH_4 + H_2) gas mixtures with THF aqueous solution are shown in Figs. 11 and 12, and are consistent with experimental data (Tables 3–5).

The calculated results for systems containing hydrogen and nitrogen are depicted in Figs. 13 and 14. The predictions match the experimental data well (Tables 6 and 7).

Regarding systems containing THF, the average calculation deviation is greater than that for systems containing pure water, especially when high concentrations of THF are used. This is because both water and THF are polar substances. The calculation precision of thermodynamic properties for such substances needs to be enhanced. Moreover, it is difficult to determine experimentally the composition of a gas mixture in the hydrate phase, making it hard to test the calculation model.

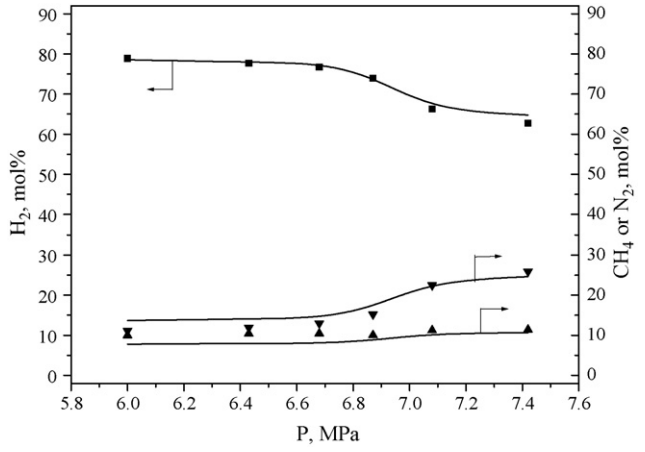

Fig. 13. Comparison of calculated and experimental composition of a (H_2 + N_2 + CH_4) gas mixture in the vapor phase with 1 mol% THF aqueous solution (T = 274.95 K). (■) Experimental data (H_2); (▲) experimental data (N_2); (▼) experimental data (CH_4); (—) calculation results.

4. Conclusions

The hydrate formation data of a (methane + ethylene) gas mixture with THF aqueous solution were measured. They are valuable for determining the parameters of the hydrate model. The vapor–hydrate equilibrium data of systems containing methane, ethane, ethylene and hydrogen in the absence and presence of THF were measured, which is important for the separation of gas mixtures via hydrate technology.

A vdW–P-type hydrate model, the Du–Guo model, was extended to systems containing hydrogen and THF. The parameters of the hydrate model were determined by correlating the experimental data of hydrate formation conditions. The algorithm for vapor–hydrate equilibria was developed and a study of composition in the hydrate phase for a (CH_4 + C_2H_6) gas mixture was performed. It was proven that two hydrate structures coexisted under the conditions studied. We applied hydrate formation kinetics to control the ratio of the two structures in the hydrate phase. The tests show that the predicted results are consistent with the experimental data.

More work is needed regarding equilibrium calculations for systems containing the polar substance THF. The approach for measuring vapor–hydrate equilibria should be improved, which would be of great value for testing the hydrate model and algorithm.

References

[1] D.N. Glew, US Patent 3,231,630 (1966).
[2] D.F. Spencer, US Patent 6,106,595 (2000).
[3] S.P. Kang, H. Lee, Environ. Sci. Technol. 34 (2000) 4397.
[4] C.-F. Ma, G.-J. Chen, F. Wang, C.-Y. Sun, T.-M. Guo, Fluid Phase Equilibr. 191 (2001) 41–47.

[5] Y. Yamamoto, T. Komai, T. Kawamura, J.H. Yoon, S.P. Kang, S. Okita, Proceedings of the Fourth International Conference on Gas Hydrates, Yokohama, May 19–23, 2002, p. 428.
[6] A.L. Ballard, E.D. Sloan Jr., Proceedings of the Fourth International Conference on Gas Hydrates, Yokohama, May 19–23, 2002, p. 1007.
[7] J.B. Klauda, S.I. Sandler, Chem. Eng. Sci. 58 (2003) 27–41.
[8] L.-W. Zhang, G.-J. Chen, X.-Q. Guo, C.Y. Sun, L.-Y. Yang, Fluid Phase Equilibr. 225 (2004) 141–144.
[9] L.-W. Zhang, G.-J. Chen, C.-Y. Sun, S.-S. Fan, Y.-M. Ding, X.-L. Wang, L.-Y. Yang, Chem. Eng. Sci. 60 (2005) 5356.
[10] Y.-H. Du, T.-M. Guo, Acta Petrol. Sin. 4 (3) (1988) 82–92.
[11] Y.-X. Zuo, S. Commesen, T.-M. Guo, Proceedings of the Second International Symposium on Thermodynamics in Chemical Engineering and Industry, Beijing, 1994.
[12] N.C. Patel, A.S. Teja, Chem. Eng. Sci. 37 (3) (1982) 463–473.
[13] S. Subramanian, A.L. Ballard, R.A. Kini, S.F. Dec, E.D. Sloan Jr., Chem. Eng. Sci. 55 (2000) 5763–5771.
[14] A.L. Ballard, E.D. Sloan Jr., Chem. Eng. Sci. 55 (2000) 5773–5782.
[15] S.-S. Fan, T.-M. Guo, J. Chem. Eng. Data 44 (1999) 829–832.
[16] D.-H. Mei, J. Liao, J.-T. Yang, T.-M. Guo, J. Chem. Eng. Data 43 (1998) 178–182.
[17] S.-X. Zhang, G.-J. Chen, C.-F. Ma, L.-Y. Yang, T.-M. Guo, J. Chem. Eng. Data 45 (2000) 908–911.
[18] Q. Zhang, G.-J. Chen, Q. Huang, C.-Y. Sun, X.-Q. Guo, Q.-L. Ma, J. Chem. Eng. Data 50 (2005) 234.
[19] J.A. van der Waals, J.C. Platteeuw, Adv. Chem. Phys. 2 (1959) 2–57.
[20] Y.-H. Du, T.-M. Guo, Chem. Eng. Sci. 45 (4) (1990) 893–900.
[21] Z. Yang, T.M. Guo, Nat. Gas Ind. (in Chinese) 16 (4) (1996) 60–65.
[22] G.M. Wilson, J. Am. Chem. Soc. 86 (1964) 127–130.
[23] J. de Graauw, J.J. Rutten, Proceedings of the Third International Symposium on Fresh Water from the Sea, vol. 3, Amaroussion, Athens, 1970, pp. 103–116.
[24] P. Skovborg, H.J. Ng, P. Rasmussen, Chem. Eng. Sci. 48 (1993) 445–453.
[25] W.M. Deaton, E.M. Frost Jr., The U.S. Bureau of Mines, Monograph 8, 1964.
[26] S.-X. Zhang, G.-J. Chen, L.-Y. Yang, C.-F. Ma, T.-M. Guo, J. Chem. Ind. Eng. (in Chinese) 54 (1) (2003) 24–28.